Isodoublet vector leptoquark solution to the muon $g-2$, R_{K,K^*}, R_{D,D^*}, and W-mass anomalies

Kingman Cheung,[1,2] Wai-Yee Keung,[3] and Po-Yan Tseng[1]
[1]*Department of Physics and CTC, National Tsing Hua University, Hsinchu 300, Taiwan*
[2]*Division of Quantum Phases and Devices, School of Physics, Konkuk University, Seoul 143-701, Republic of Korea*
[3]*Department of Physics, University of Illinois at Chicago, Illinois 60607, USA*

(Received 25 May 2022; accepted 20 July 2022; published 28 July 2022)

We investigate the isodoublet vector leptoquark V_2 as a solution to the B anomalies R_{K,K^*} and R_{D,D^*}, as well as explaining the muon and electron anomalous magnetic moments and the very recent W-mass anomaly.

DOI: 10.1103/PhysRevD.106.015029

I. INTRODUCTION

Recent trends in hunting for new physics beyond the standard model (SM) can divided into (i) high-energy frontier, (ii) precision frontier, and (iii) cosmology frontier. While the high-energy frontier has not been finding anything new other than the discovery of the Higgs boson and the cosmology frontier involves large uncertainties associated with observations, the precision frontier, on the other hand, has shown some surprising results. Namely, there are a number of anomalies in B meson decays, the muon anomalous moment, and the very recent W-boson mass measurement [1].

After accumulating data for a number of years, there exist persistent discrepancies between the SM predictions and the experimental results for the flavor-changing neutral current rare decays of B mesons in $b \to s\ell\ell$. In particular, the lepton-flavor universality violation in $B \to K$ transition observed by LHCb

$$R_K = \frac{\mathrm{BR}(B \to K\mu^+\mu^-)}{\mathrm{BR}(B \to Ke^+e^-)}, \qquad R_{K*} = \frac{\mathrm{BR}(B \to K^*\mu^+\mu^-)}{\mathrm{BR}(B \to K^*e^+e^-)}, \tag{1.1}$$

with the measurements [2,3]

$$R_K = 0.846^{+0.042\ +0.013}_{-0.039\ -0.012} \quad \text{for } 1.1\ \mathrm{GeV}^2 < q^2 < 6\ \mathrm{GeV}^2, \tag{1.2}$$

$$R_{K^*} = \begin{cases} 0.66^{+0.11}_{-0.07} \pm 0.03 & 0.045\ \mathrm{GeV}^2 < q^2 < 1.1\ \mathrm{GeV}^2, \\ 0.69^{+0.11}_{-0.07} \pm 0.05 & 1.1\ \mathrm{GeV}^2 < q^2 < 6.0\ \mathrm{GeV}^2, \end{cases} \tag{1.3}$$

which deviate from the SM predictions by as much as 3σ. The advantage of using ratios is that the ratio can have a lot of hadronic uncertainties in each branching ratio measurement to be eliminated. Precise measurements of these ratios with significant deviations from the SM predictions can hint at new physics. The same short-distance process $b \to s\ell\ell$ is also responsible for $B_s^0 \to \ell^+\ell^-$.

Another set of observables is related to the short-distance process $b \to c\ell\nu$, and the observables are [4]

$$R_D = \frac{\mathrm{BR}(B \to D\tau\nu)}{\mathrm{BR}(B \to D\ell\nu)} = 0.340 \pm 0.027 \pm 0.013,$$
$$R_{D^*} = \frac{\mathrm{BR}(B \to D^*\tau\nu)}{\mathrm{BR}(B \to D^*\ell\nu)} = 0.295 \pm 0.011 \pm 0.008, \tag{1.4}$$

and the combined discrepancy to SM prediction is at the 3.1σ level.

Another long-standing experimental anomaly is the muon anomalous moment (also known as $g-2$). The most recent muon $g-2$ measurement was performed by the E989 experiment at Fermilab, which reported the new result [5]

$$\Delta a_\mu = (25.1 \pm 5.9) \times 10^{-10}, \tag{1.5}$$

which deviates at the level of 4.2σ from the most recent SM prediction.[1] On the other hand, the $g-2$ measurements for

[1]There was a recent lattice calculation of the leading hadronic contribution to the muon magnetic moment [6], which brought the SM prediction within 1σ of the experimental result. Yet, one has to wait further for the lattice community to settle on the calculation. We will focus on Eq. (3.6) for the deviation of muon $g-2$.

the electron also show a discrepancy with the SM prediction. The electron $g-2$ was used to be the most precise determination of the fine-structure constant α. Nevertheless, there were two contradicting determinations of α [7,8] resulting in two theory predictions, which deviate from the experimental measurement [9] in opposite directions, given by

$$\Delta a_e^{\mathrm{LKB}} = a_e^{\mathrm{exp}} - a_e^{\mathrm{LKB}} = (4.8 \pm 3.0) \times 10^{-13},$$
$$\Delta a_e^{\mathrm{B}} = a_e^{\mathrm{exp}} - a_e^{\mathrm{B}} = (-8.8 \pm 3.6) \times 10^{-13}. \quad (1.6)$$

In the following analysis, we show the results for both cases of Δa_e. Note that, if we want to explain the Δa_μ with new physics, it is very likely subject to constraints coming from lepton-flavor-violating (LFV) decays, such as $\mu \to e\gamma$.

There has been a vast literature in explaining all or part of the anomalies. Especially, the leptoquark (LQ) provides viable explanations for the R_{K,K^*} and/or R_{D,D^*} anomalies. It was illustrated in Ref. [10] that only the isosinglet vector LQ U_1 with the SM quantum numbers $(\mathbf{3},\mathbf{1},2/3)$ can explain both R_{K,K^*} and R_{D,D^*}, while the scalar LQs S_1, S_3, and R_2 and the isotriplet vector LQ $U_3(\mathbf{3},\mathbf{1},2/3)$ can explain only one of the anomalies. There have been very few studies on the isospin-doublet vector LQ, denoted by $V_2(\mathbf{3},\mathbf{2},5/6)$. In this work, we attempt to fill the gap by showing that the isodoublet vector LQ V_2 can satisfy the anomalies R_{K,K^*} and R_{D,D^*}, as well as it can satisfy the Δa_μ and Δa_e subject to LFV constraints.

Very recently, there was a new W-boson mass measurement by the CDF Collaboration [1]:

$$M_W = 80.4335 \pm 0.0094 \text{ GeV},$$

which is about 7σ above the SM prediction of $M_{W,\mathrm{SM}} = 80.361 \pm 0.006$ GeV [11]. Additional corrections to the W-boson mass can come from new physics, which can be conveniently parametrized in terms of the Peskin-Takeuchi parameters S, T, and U [12]. The W-boson mass correction is most sensitive to the T parameter. It is well known that an electroweak doublet with a mass splitting between the upper and lower components contributes positively to the T parameter and, thus, gives a positive contribution to the W mass.

We highlight the capabilities of the LQ V_2 in solving the anomalies.

(1) The more popular explanation of the R_{K,K^*} anomaly is by decreasing the $b \to s\mu^+\mu^-$ using the left-handed coupling to the muon, such that the combination of the Wilson coefficients C_9 and C_{10} is in the form $C_9 = -C_{10}$ in accordance with the best fit [13]. This is the case of the isosinglet vector LQ U_1, On the other hand, the isodoublet vector LQ V_2 couples to the right-handed lepton. such that it contributes to C_9 and C_{10} in the combination of $C_9 = C_{10}$. We, therefore, require V_2 to couple to the electron and to increase $b \to se^+e^-$.
(2) V_2 can enhance substantially the Δa_μ and change Δa_e in both directions using different combinations of couplings. Nevertheless, in order to reach with 2σ of Δa_μ, one of the couplings has to be very large. This is due to the constraint from the $\mu \to e\gamma$.
(3) R_{D,D^*} can be easily satisfied.
(4) The isodoublet LQ V_2 can couple to the weak gauge bosons and, thus, modifies the S, T, and U parameters. It can explain the very recent W-mass anomaly measured by CDF.

The organization of this work is as follows. In the next section, we introduce the interactions of the vector LQ. In Sec. III, we describe the effects of the vector LQ on various observables that we used in this analysis. In Sec. IV, we give the results and the valid parameter space. We conclude in Sec. V.

II. VECTOR LEPTOQUARK INTERACTIONS

The weak isodoublet vector LQ is denoted by V_2 with the SM quantum numbers $(\bar{\mathbf{3}},\mathbf{2},5/6)$. The V_2 is written as

$$V_2 = \begin{pmatrix} V^{+4/3} \\ V^{+1/3} \end{pmatrix}.$$

For simplicity, we drop the subscript of V_2 from now on. The gauge interaction of the V_2 is given by

$$\mathcal{L}_{V_2} = -\frac{1}{2}V^\dagger_{\mu\nu}V^{\mu\nu} + M_V^2 V^\dagger_\mu V^\mu + ig_3 V^\dagger_\mu \frac{\lambda^A}{2} V_\nu G^{A,\mu\nu} + ig_2 V^\dagger_\mu \frac{\tau^k}{2} V_\nu W^{k,\mu\nu} + ig_1 V^\dagger_\mu Y V_\nu B^{\mu\nu}, \quad (2.1)$$

where $V_{\mu\nu} = \sum_{i=1,2} D_\mu V^i_\nu - D_\nu V^i_\mu$ and

$$D_\mu = \partial_\mu + ig_1 Y B_\mu + ig_2 \frac{\tau^k}{2} W^k_\mu + ig_3 \frac{\lambda^A}{2} G^A_\mu, \quad (2.2)$$

where the $SU(2)_L$ index $k = 1, 2, 3$ and the color index $A = 1, \ldots, 8$.[2] In order to extract the electromagnetic interaction with V_2, we transform B_μ and W^3_μ into A_μ and Z_μ by the usual transformation:

$$B_\mu = c_w A_\mu - s_w Z_\mu, \qquad W^3_\mu = s_w A_\mu + c_w Z_\mu,$$

where $c_w = \cos\theta_W$, $s_w = \sin\theta_W$, and θ_W is the weak mixing angle. As long as the electromagnetic interaction is concerned, we simplify the Lagrangian as

[2]Here, we have taken all $\kappa = 1$ and $\tilde{\kappa} = 0$ as in the convention of Ref. [14] with the assumption of V_2 coming from spontaneous breakdown of a gauge symmetry. Note the major difference is that U_1 discussed in Ref. [14] always connects down-type quarks and charged leptons of the same chiralities, while here the V_2 always connects them with opposite chiralities.

$$\mathcal{L}_{V_2,\mathrm{em}} = -\frac{1}{2}V^{\dagger}_{\mu\nu}V^{\mu\nu} + ieQ_V V^{\dagger}_{\mu}V_{\nu}F^{\mu\nu} + \cdots, \tag{2.3}$$

where $D_\mu = \partial_\mu + ieQ_V A_\mu + \cdots$. Extracting the triple vertex $V^\dagger VA$, we obtain

$$\begin{aligned}\mathcal{L}_{V^\dagger VA} &= -\frac{1}{2}[ieQ_V(\partial_\mu V^{\dagger}_{\nu} - \partial_\nu V^{\dagger}_{\mu})(A^\mu V^\nu - A^\nu V^\mu) - ieQ_V(A_\mu V^{\dagger}_{\nu} - A_\nu V^{\dagger}_{\mu})(\partial^\mu V^\nu - \partial^\nu V^\mu)] + ieQ_V V^{\dagger}_{\mu}V_\nu(\partial^\mu A^\nu - \partial^\nu A^\mu)\\ &= -ieQ_V(\partial_\mu V^{\dagger}_{\nu} - \partial_\nu V^{\dagger}_{\mu})A^\mu V^\nu + ieQ_V A_\mu V^{\dagger}_{\nu}(\partial^\mu V^\nu - \partial^\nu V^\mu) + ieQ_V V^{\dagger}_{\mu}V_\nu(\partial^\mu A^\nu - \partial^\nu A^\mu).\end{aligned}$$

We assign the 4-momenta and polarization vectors for $V^\dagger$, V, and A as, respectively,

$$V^\dagger\colon\ p',\lambda'; \qquad V\colon\ p,\lambda; \qquad A\colon\ k,\epsilon.$$

Then we obtain the triple vertex as

$$\begin{aligned}\mathcal{L}_{V^\dagger VA} &= eQ_V[g_{\alpha\beta}(p-p')_\gamma + g_{\beta\gamma}(p'-k)_\alpha\\ &\quad + g_{\gamma\alpha}(k-p)_\beta]\lambda^\alpha\lambda'^\beta\epsilon^\gamma.\end{aligned} \tag{2.4}$$

Therefore, the interaction of V with the photon is the same as the conventional charged vector boson.

The interactions of V_2 with SM fermions are given by[3]

$$\begin{aligned}\mathcal{L}_{Vff} &= X^{RL}_{ij}\epsilon^{ab}\overline{d^{c,i}_R}\gamma^\mu V^a_\mu L^{j,b}_L + X^{LR}_{ij}\epsilon^{ab}\overline{Q^{c,i,a}_L}\gamma^\mu V^b_\mu e^j_R + \mathrm{H.c.}\\ &= X^{RL}_{ij}[\overline{d^{c,i}_R}\gamma^\mu \ell^j_L V^{+4/3}_\mu - \overline{d^{c,i}_R}\gamma^\mu \nu^j_L V^{+1/3}_\mu]\\ &\quad + X^{LR}_{ij}[\overline{u^{c,i}_L}\gamma^\mu e^j_R V^{+1/3}_\mu - \overline{d^{c,i}_L}\gamma^\mu e^j_R V^{+4/3}_\mu] + \mathrm{H.c.},\end{aligned} \tag{2.5}$$

where we assume that the down-type quarks and charged leptons are in the mass eigenstates while the Cabibbo-Kobayashi-Maskawa (CKM) matrix is associated with the up-type quarks. To convert the up-type quarks of the interaction basis in Eq. (2.5) into the mass eigenstates, we need to replace $\overline{u^{c,i}_L}$ in Eq. (2.5) by $V_{ij}\overline{u^{c,i}_L}$ via CKM matrix V_{ij}.

III. VARIOUS OBSERVABLES

In this section, we summarize various observables that we are going to include in this analysis, namely, the muon anomalous magnetic moment (also known as $g-2$) and lepton-flavor-violating radiative decays and B anomalies R_{K,K^*} and R_{D,D^*}. The W-boson mass is accounted for by the mass splitting the isospin components of the V_2, which has negligible effects on the low-energy observables.

[3]In principle, there could be diquark couplings to V_2, but they would lead to dangerous proton decay [15]. Therefore, we do not include them here.

A. $g-2$ and $\ell_i \to \ell_j\gamma$

The amplitudes for the lepton anomalous magnetic moment Δa_ℓ and lepton-flavor-violating radiative decays $\ell_i \to \ell_j\gamma$ are related. We can write the transition amplitude for

$$\ell_i(p) \to \ell_j(p-q)\gamma(q),$$

where the 4-momentum p is coming and q is outgoing, as

$$T = e\epsilon^{\mu *}(q)m_{\ell_i}\bar{u}(p-q)i\sigma_{\mu\nu}q^\nu[A^{\ell_i\ell_j}_L P_L + A^{\ell_i\ell_j}_R P_R]u(p). \tag{3.1}$$

Then, the partial width of $\Gamma(\ell_i \to \ell_j\gamma)$ can be expressed as

$$\Gamma(\ell_i \to \ell_j\gamma) = \frac{\alpha_{\mathrm{em}}}{4}m^5_{\ell_i}(|A^{\ell_i\ell_j}_L|^2 + |A^{\ell_i\ell_j}_R|^2), \tag{3.2}$$

where the mass of the daughter lepton ℓ_j is ignored.

On the other hand, the anomalous magnetic moment form factor of the lepton ℓ is given by

$$\begin{aligned}\mathcal{L}_{g-2} &= \frac{e\Delta a_\ell}{4m_\ell}\bar{\ell}\sigma_{\mu\nu}\ell F^{\mu\nu}\\ &= \frac{e\Delta a_\ell}{2m_\ell}\bar{\ell}i\sigma_{\mu\nu}(q^\nu)\ell A^\mu,\end{aligned} \tag{3.3}$$

where Δa_ℓ is the anomalous magnetic moment of the lepton and here q is coming into the vertex. Comparing Eqs. (3.1) and (3.3), we have

$$\Delta a_\ell = -m^2_\ell(A^{\ell\ell}_L + A^{\ell\ell}_R). \tag{3.4}$$

We adopted the formulas here from Ref. [16] for $\ell_i \to \ell_j\gamma$:

$$\begin{aligned}A^{\ell_i\ell_j}_L &= -\frac{N_C}{16\pi^2 M^2_V}\sum_k\left[-2X^{LR*}_{k\ell_j}X^{RL}_{k\ell_i}\frac{m_k}{m_{\ell_i}}(Q_V + Q_{b^c})\right.\\ &\quad \left. + \left(X^{LR*}_{k\ell_j}X^{LR}_{k\ell_i} + X^{RL*}_{k\ell_j}X^{RL}_{k\ell_i}\frac{m_{\ell_j}}{m_{\ell_i}}\right)\left(-\frac{5}{6}Q_V - \frac{2}{3}Q_{b^c}\right)\right],\\ A^{\ell_i\ell_j}_R &= A^{\ell_i\ell_j}_L(L \leftrightarrow R),\end{aligned} \tag{3.5}$$

where $Q_{b^c} = -Q_b$ denotes the electric charge of the charge conjugate of the b quark and $Q_V = +4/3$ refers to the upper component of V_2. We have made use of the fact that

all down-type quark masses are much smaller than the LQ mass $m_k/M_V \ll 1$ such that the loop functions f, g, h, and j approach constant values [16].

We can express the contribution of the LQ to the lepton anomalous moment as

$$\Delta a_\ell = -\frac{N_C}{16\pi^2}\left[4\mathcal{R}e(X^{LR*}_{3\ell}X^{RL}_{3\ell})\frac{m_b m_\ell}{M_V^2}(Q_V+Q_{b^c}) + 2(|X^{LR}_{3\ell}|^2+|X^{RL}_{3\ell}|^2)\frac{m_\ell^2}{M_V^2}\left(\frac{5}{6}Q_V+\frac{2}{3}Q_{b^c}\right)\right], \quad (3.6)$$

where we assume that the contribution from the b quark dominates over the s and d quarks. The partial width for the radiative decay, such as $\mu \to e\gamma$, is given by

$$\Gamma(\mu \to e\gamma) = \frac{\alpha_{\rm em}}{4} m_\mu^5 (|A_L^{\mu e}|^2 + |A_R^{\mu e}|^2). \quad (3.7)$$

B. R_{K,K^*}

The effective Lagrangian for a generic exclusive decay of $b \to s\ell^-\ell^+$, with $\ell = e, \mu, \tau$, can be written as

$$\mathcal{L}_{bs\ell\ell} \supset \frac{4G_F}{\sqrt{2}} V_{tb}V_{ts}^* \frac{e^2}{16\pi^2}\sum_i [C_i\mathcal{O}_i + C_i'\mathcal{O}_i'] + \text{H.c.}, \quad (3.8)$$

where

$$\mathcal{O}_9 = (\bar{s}\gamma_\mu P_L b)(\bar{\ell}\gamma^\mu \ell), \qquad \mathcal{O}_9' = (\bar{s}\gamma_\mu P_R b)(\bar{\ell}\gamma^\mu \ell),$$
$$\mathcal{O}_{10} = (\bar{s}\gamma_\mu P_L b)(\bar{\ell}\gamma^\mu\gamma^5 \ell), \qquad \mathcal{O}_{10}' = (\bar{s}\gamma_\mu P_R b)(\bar{\ell}\gamma^\mu\gamma^5 \ell),$$
$$\mathcal{O}_S = (\bar{s}P_R b)(\bar{\ell}\ell), \qquad \mathcal{O}_S' = (\bar{s}P_L b)(\bar{\ell}\ell),$$
$$\mathcal{O}_P = (\bar{s}P_R b)(\bar{\ell}\gamma_5 \ell), \qquad \mathcal{O}_P' = (\bar{s}P_L b)(\bar{\ell}\gamma_5 \ell).$$

Since the term responsible for the left-handed down-type quark V_2 interaction is $-X^{LR}_{ij}\overline{d_L^{c,i}}\gamma^\mu e_R^j V_\mu^{+4/3}$, which involves only the right-handed charged lepton e_R^j, it will give rise to the relation $C_9 = C_{10}$ between C_9 and C_{10}. Therefore, we focus on the interactions with the electron instead of the muon, as the best-fit results preferred $C_9 = -C_{10}$ for the muon but $C_9 = +C_{10}$ for the electron. The contributions to the Wilson coefficients from V_2 focusing on the interactions with the electron are given by

$$C_9^{bsee} = +C_{10}^{bsee} = -\frac{4\pi^2}{e^2}\frac{v^2}{M_{V_2}^2}\frac{X_{31}^{LR}X_{21}^{LR*}}{V_{ts}^*V_{tb}},$$
$$C_9'^{bsee} = -C_{10}'^{bsee} = -\frac{4\pi^2}{e^2}\frac{v^2}{M_{V_2}^2}\frac{X_{31}^{RL}X_{21}^{RL*}}{V_{ts}^*V_{tb}},$$
$$C_S^{bsee} = -C_P^{bsee} = \frac{4\pi^2}{e^2}\frac{2v^2}{M_{V_2}^2}\frac{X_{31}^{RL}X_{21}^{LR*}}{V_{ts}^*V_{tb}},$$
$$C_S'^{bsee} = +C_P'^{bsee} = \frac{4\pi^2}{e^2}\frac{2v^2}{M_{V_2}^2}\frac{X_{31}^{LR}X_{21}^{RL*}}{V_{ts}^*V_{tb}}.$$

Strictly speaking, the above Wilson coefficients are calculated at the electroweak scale by integrating out the heavy degrees of freedom such as the LQ. One has to evolve them down to the m_b scale. However, given that the evolution effect is very small because of small mixings between the operators and $\mathcal{O}_2 \equiv (\bar{s}\gamma_\mu(1-\gamma_5)c)(\bar{c}\gamma^\mu(1-\gamma_5)b)$,[4] we directly employ the above expressions in our analysis, similarly for the Wilson coefficient C_{S_R}.

C. R_{D,D^*}

The effective Lagrangian for a generic exclusive decay of $b \to c\tau^-\bar{\nu}_\tau$ can be written as

$$\mathcal{L}_{bc\ell\nu} = -2\sqrt{2}G_F V_{cb}[(1+C_{V_L})(\overline{c_L}\gamma^\mu b_L)(\overline{\tau}\gamma^\mu \nu_{\tau_L}) + C_{V_R}(\overline{c_R}\gamma^\mu b_R)(\overline{\tau}\gamma^\mu\nu_{\tau_L}) + C_{S_R}(\overline{c_L}b_R)(\overline{\tau}\nu_{\tau_L}) + C_{S_L}(\overline{c_R}b_L)(\overline{\tau}\nu_{\tau_L}) + C_T(\overline{c_R}\sigma^{\mu\nu}b_L)(\overline{\tau}\sigma_{\mu\nu}\nu_{\tau_L})]. \quad (3.9)$$

The isospin $-1/2$ component of the V_2 contributes to the process $b \to c\tau\nu_\tau$ via the operator $(\overline{c_L}b_R)(\overline{\tau}\nu_{\tau_L})$ and, thus, modifies the coefficient C_{S_R}:

$$C_{S_R} = -\frac{1}{2\sqrt{2}G_F}\frac{1}{V_{cb}}\sum_k\left(V_{k2}\frac{2}{M_V^2}X_{33}^{RL}X_{k3}^{LR*}\right). \quad (3.10)$$

D. $B_s \to \ell^+\ell^-$

Including the new physics contributions, the general expression of the $B_s \to \ell^+\ell^-$ in terms of Wilson coefficients is [17]

$$\text{Br}(B_s \to \ell^+\ell^-) = \tau_{B_s} f_{B_s}^2 m_{B_s}^3 \frac{G_F^2|V_{tb}V_{ts}^*|^2 e^4}{(4\pi)^5}\sqrt{1-4m_\ell^2/m_{B_s}^2}\left[\frac{m_{B_s}^2}{m_b^2}|C_S - C_S'|^2\left(1-\frac{4m_\ell^2}{m_{B_s}^2}\right) + \left|\frac{m_{B_s}}{m_b}(C_P - C_P') + \frac{2m_\ell}{m_{B_s}}(C_{10}^{\rm SM} + C_{10} - C_{10}')\right|^2\right], \quad (3.11)$$

[4]We especially thank Wolfgang Altmannshofer for explaining this point.

where $C_{10}^{\rm SM} = -4.1$ stems from the SM contribution and $\tau_{B_s} = 1.52 \times 10^{-12}$ s and $f_{B_s} = 228.4$ MeV are the lifetime and decay constant of the B meson, respectively. The current measurements are [13]

$$\mathrm{Br}(B_s \to \mu^+\mu^-) = (3.09^{+0.48}_{-0.44}) \times 10^{-9}, \quad (3.12)$$

$$\mathrm{Br}(B_s \to e^+e^-) < 9.4 \times 10^{-9} \quad \text{at } 90\% \text{ C.L. from PDG}, \quad (3.13)$$

and consistent with the SM.

E. W-boson mass

The W-boson mass due to new physics expressed in terms of the ΔS, ΔT, and ΔU is given by

$$M_W^2 = M_{W,\mathrm{SM}}^2 + \frac{\alpha c_W^2 M_Z^2}{c_W^2 - s_W^2}\left[-\frac{\Delta S}{2} + c_W^2 \Delta T + \frac{c_W^2 - s_W^2}{4 s_W^2}\Delta U\right], \quad (3.14)$$

where c_W and s_W are, respectively, the cosine and the sine of the Weinberg angle. α is the fine-structure constant, and M_Z is the Z-boson mass. In the SM, $M_{W,\mathrm{SM}} = 80.361 \pm 0.006$ GeV [11], while the most recent measurement by CDF is $M_W = 80.4335 \pm 0.0094$ GeV [1]. Such a large deviation can be most easily accommodated by a positive ΔT. It is well known that an additional weak doublet with a mass splitting gives a contribution to ΔT as[5]

$$\Delta T = \frac{C}{4\pi M_W^2 s_W^2} F(m_1, m_2), \quad (3.15)$$

where $C = 1$ (3) for a color singlet (triplet) and

$$F(m_1, m_2) = m_1^2 + m_2^2 - \frac{2 m_1^2 m_2^2}{m_1^2 - m_2^2}\log\left(\frac{m_1^2}{m_2^2}\right).$$

Note that ΔT is proportional to the mass splitting $\Delta m = |m_1 - m_2|$ between the upper and the lower component of the doublet and, thus, always positive. With this ΔT, the change in M_W^2 is given by

$$\Delta M_W^2 = \frac{\alpha c_W^4 M_Z^2}{c_W^2 - s_W^2}\Delta T. \quad (3.16)$$

TABLE I. Best-fitted results of the relevant Wilson coefficients for R_{K,K^*} [13] and R_{D,D^*} [19], muon and electron anomalous magnetic moments Δa_μ [5] and Δa_e [7–9]. Note that there is a controversy for Δa_e due to two different experimental measurements.

$C_9^{bsee} = C_{10}^{bsee}$	$-1.28^{+0.24}_{-0.23}$
$C_{S_R}^{\ell}$	$0.027^{+0.025}_{-0.026}$
Δa_μ	$(251 \pm 59) \times 10^{-11}$
$\Delta a_e^{\mathrm{LKB}}$	$(4.8 \pm 3.0) \times 10^{-13}$
Δa_e^{B}	$(-8.8 \pm 3.6) \times 10^{-13}$

IV. PARAMETER SCANS AND RESULTS

The best-fitted results on the Wilson coefficients were updated in early 2021 [13]. We list them in Table I. The LQ couplings can involve different leptonic flavors in the same Feynman diagram, and so it will also give rise to the lepton-flavor-violating processes, notably, the radiative leptonic decays $\ell_i \to \ell_j \gamma$. While these processes have not been observed, the upper limits are quite restrictive:

$$B(\tau \to \mu\gamma) < 4.4 \times 10^{-8}, \quad 90\%\,\text{C.L.},$$
$$B(\tau \to e\gamma) < 3.3 \times 10^{-8}, \quad 90\%\,\text{C.L.},$$
$$B(\mu \to e\gamma) < 4.2 \times 10^{-13}, \quad 90\%\,\text{C.L.}$$

We perform the global chi-square fit to the observables, including R_{K,K^*}, R_{D,D^*}, $B_s \to \ell^+\ell^-$, and $\ell_i \to \ell_j\gamma$, by scanning the couplings of LQ V_2 with the scanning ranges of various couplings:

$$\begin{aligned}\text{Scan:}\ & -20 \le X_{21}^{\mathrm{LR}} \le 20, \quad 0 \le X_{31}^{\mathrm{LR}} \le \sqrt{4\pi}, \quad -1 \le X_{31}^{\mathrm{RL}} \le 1,\\ & -\sqrt{4\pi} \le X_{22}^{\mathrm{LR}} \le \sqrt{4\pi}, \quad -2\sqrt{4\pi} \le X_{32}^{\mathrm{LR}} \le 2\sqrt{4\pi}, \quad -1 \le X_{32}^{\mathrm{RL}} \le 1,\\ & -1 \le X_{23}^{\mathrm{LR}} \le 1, \quad -2 \le X_{33}^{\mathrm{RL}} \le 2, \quad m_{V_2} = 2\ \text{TeV}.\end{aligned} \quad (4.1)$$

Since the theoretical uncertainties are still ambiguous among $\Delta a_{e,\mu}$, we have not included the observables in the global fit at this stage but rather treat them as posterior predictions. Because of the facts that all the observables and Wilson coefficients are originated from products of two couplings, such that only the relative sign between couplings would be revealed from the chi-square fitting, we scanned the positive value of X_{31}^{LR} and both signs for the other couplings. Note that the X_{21}^{LR} and $X_{31}^{\mathrm{LR,RL}}$ (X_{22}^{LR} and

[5]This expression is based on the formulas listed in Appendix D of Pokorski's book [18].

$X_{32}^{\mathrm{LR,RL}}$) are related to $C_{9,10}^{bsee}$ ($C_{9,10}^{bs\mu\mu}$). The X_{23}^{LR} combining with $X_{3\ell}^{\mathrm{RL}}$ dominantly contributes to $C_{S_R}^{\ell}$, while other combinations are suppressed due to the off-diagonal elements of the CKM matrix. Since the flavors of neutrino are indistinguishable in the process $b \to c\tau\nu_\ell$, we sum over the neutrino flavors. The Δa_e (Δa_μ) are generated through a pair of bottom quark and V_2 running in the loop, since the heavy b-quark mass enhances flipping the chiralities of external muons; thereby, they are strongly correlated to $X_{31}^{\mathrm{LR,RL}}$ ($X_{32}^{\mathrm{LR,RL}}$). We adopted the two-dimensional chi-square statistics; i.e., $\Delta\chi^2 \leq 2.30$ (6.18) corresponds to 1σ (2σ) regions. The chi-square distributions are shown in Fig. 1,

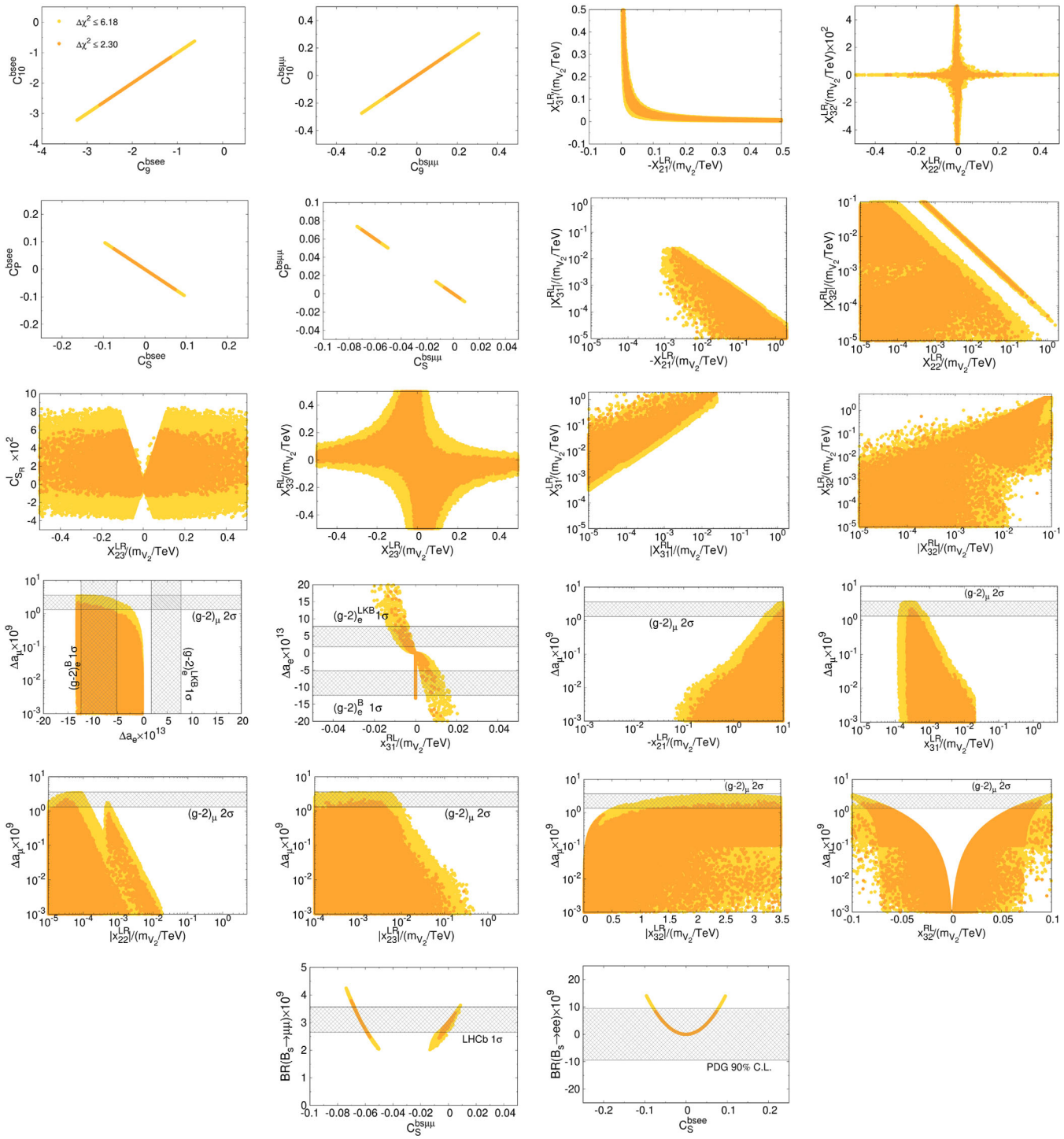

FIG. 1. Scan: The chi-square distribution includes R_{K,K^*}, R_{D,D^*}, $B_s \to \ell^+\ell^-$, and $\ell_j \to \ell_i\gamma$ data. The best-fit point, BP-1, gives $\chi^2|_{R_K+R_D+B_s+\mathrm{LFV}} = 22.48$ with pull 3.8σ compared to the SM, $\chi^2|_{R_K+R_D+B_s+\mathrm{LFV}} = 36.92$.

TABLE II. Benchmark points with $m_{V_2} = 2$ TeV. The SM gives $\chi^2|_{R_K+R_D+B_s+\mathrm{LFV}} = 36.92$, $\chi^2|_{R_K+R_D+\mathrm{LFV}+a_\mu+a_e^{\mathrm{LKB}}} = 57.58$, and $\chi^2|_{R_K+R_D+\mathrm{LFV}+B_s+a_\mu+a_e^{\mathrm{B}}} = 61.00$.

	BP-1	BP-2	BP-3
X_{21}^{LR}	-0.445	-17.85	-0.0115
X_{31}^{LR}	0.0271	6.44×10^{-4}	0.927
X_{31}^{RL}	1.58×10^{-4}	-2.48×10^{-8}	-0.0145
X_{22}^{LR}	-0.0245	-7.18×10^{-5}	-0.0606
X_{32}^{LR}	-2.01×10^{-3}	6.820	1.11×10^{-5}
X_{32}^{RL}	-8.25×10^{-3}	-0.183	-1.19×10^{-5}
X_{23}^{LR}	-0.367	-2.35×10^{-3}	0.990
X_{33}^{RL}	0.217	-1.87×10^{-4}	-0.0252
$C_9^{bs\mu\mu} = C_{10}^{bs\mu\mu}$	7.77×10^{-3}	-7.73×10^{-3}	-1.06×10^{-4}
$C_9^{bsee} = C_{10}^{bsee}$	-1.90	-1.82	-1.68
$C_{S_R}^{\ell}$	0.0276	-1.55×10^{-4}	0.0141
$C_S^{bs\mu\mu} = -C_P^{bs\mu\mu}$	-0.0638	-4.14×10^{-3}	-2.27×10^{-4}
$C_S^{bsee} = -C_P^{bsee}$	0.0222	-1.40×10^{-4}	-0.053
$\Delta a_\mu^{V_2}$	-2.11×10^{-13}	2.12×10^{-9}	-5.19×10^{-13}
$\Delta a_e^{V_2}$	-8.02×10^{-16}	-1.05×10^{-12}	4.52×10^{-13}
$\mathrm{Br}(\tau \to \mu\gamma)$	3.36×10^{-11}	7.94×10^{-12}	2.04×10^{-9}
$\mathrm{Br}(\tau \to e\gamma)$	1.86×10^{-8}	1.01×10^{-9}	3.65×10^{-9}
$\mathrm{Br}(\mu \to e\gamma)$	1.27×10^{-13}	6.37×10^{-14}	8.68×10^{-14}
$\chi^2\|_{R_K}$	21.34	22.15	21.63
$\chi^2\|_{R_D}$	0.001	1.09	0.245
$\chi^2\|_{B_s\to\mu\mu}$	0.002	0.567	0.0408
$\chi^2\|_{B_s\to ee}$	0.018	0.000	0.548
$\chi^2\|_{\mathrm{LFV}}$	1.12	0.065	0.156
$\chi^2\|_{a_\mu}$	18.10	0.434	18.11
$\chi^2\|_{a_e^{\mathrm{LKB}}}$	2.57	26.12	0.009
$\chi^2\|_{a_e^{\mathrm{B}}}$	5.96	0.232	13.69
$\chi^2\|_{R_K+R_D+B_s+\mathrm{LFV}}$	22.48	23.88	22.62
$\chi^2\|_{R_K+R_D+B_s+\mathrm{LFV}+a_\mu+a_e^{\mathrm{LKB}}}$	43.15	50.43	40.74
$\chi^2\|_{R_K+R_D+B_s+\mathrm{LFV}+a_\mu+a_e^{\mathrm{B}}}$	46.54	24.54	54.42
$\chi^2\|_{R_K+R_D+B_s+\mathrm{LFV}+a_e^{\mathrm{LKB}}}$	25.05	50.00	22.63
$\chi^2\|_{R_K+R_D+B_s+\mathrm{LFV}+a_e^{\mathrm{B}}}$	28.44	24.11	36.31

based on projections of two selected parameters whereas marginalizing the others.

Among the scanning points using the data R_{K,K^*}, R_{D,D^*}, $B_s \to \ell^+\ell^-$, and $\ell_i \to \ell_j\gamma$, we further select three benchmark points, which yield minima of chi-square with respect to various groups of observables, and more details are listed in Table II:

(i) *BP-1*.—The best fit to R_{K,K^*}, R_{D,D^*}, $B_s \to \ell^+\ell^-$, and LFV data and gives $\chi^2|_{R_K+R_D+B_s+\mathrm{LFV}} = 22.48$ with a pull 3.8σ comparing to the SM, $\chi^2|_{R_K+R_D+B_s+\mathrm{LFV}} = 36.92$.

(ii) *BP-2*.—Gives $\chi^2|_{R_K+R_D+B_s+\mathrm{LFV}+a_\mu+a_e^{\mathrm{B}}} = 24.54$ and, thus, provides a simultaneous solution to $(g-2)_\mu$ and $(g-2)_e^{\mathrm{B}}$.

(iii) *BP-3*.—Gives $\chi^2|_{R_K+R_D+B_s+\mathrm{LFV}+a_e^{\mathrm{LKqB}}} = 22.63$ and, thus, provides an explanation for $(g-2)_e^{\mathrm{LKB}}$.

Because the isodoublet vector LQ V_2 couples to the right-handed lepton and, thus, induces $C_9^{bsee} = C_{10}^{bsee}$, the $(C_9^{bsee}, C_{10}^{bsee})$ panel in Fig. 1, the BP-1 in Table II shows that the $C_9^{bsee} = C_{10}^{bsee} = -1.90$ from V_2 provides the best solution for the R_{K,K^*} anomaly, which increases $b \to se^+e^-$ to reduce the values of R_{K,K^*}. It implies the correlation

$$\frac{X_{31}^{\mathrm{LR}}(X_{21}^{\mathrm{LR}})^*}{m_{V_2}^2} \simeq \frac{-0.0030}{(1\ \mathrm{TeV})^2} \tag{4.2}$$

and is shown in the $(-X_{21}^{\mathrm{LR}}, X_{31}^{\mathrm{LR}})$ panel in Fig. 1.

The $(X_{23}^{\mathrm{LR}}, X_{33}^{\mathrm{RL}})$ panel in Fig. 1 indicates mild correlation between $(X_{23}^{\mathrm{LR}}$ and $X_{33}^{\mathrm{RL}})$, that came from the R_{D,D^*}

observables and, thus, Wilson coefficient $C^{\ell}_{S_R}$. According to the preferred value of $C^{\ell}_{S_R}$ from Table I, Eq. (3.10) gives

$$\frac{X^{\rm RL}_{33}(X^{\rm LR}_{23})^*}{m^2_{V_2}} \simeq \frac{-0.019}{(1\ {\rm TeV})^2}, \tag{4.3}$$

where the minus sign is originated from the $V_{cd} \simeq -0.041$. Since $C^{\ell}_{S_R} = 0$ is still compatible with observation within 1σ ($\Delta\chi^2 \leq 2.3$), the chi-square regions in the $(X^{\rm LR}_{23}, X^{\rm RL}_{33})$ panel connected.

The $B_s \to \mu^+\mu^-$ observable dictates the chi-square regions in the $(C_S^{bs\mu\mu}, C_P^{bs\mu\mu})$ panel, and there are two solutions: $C_S^{bs\mu\mu} = -C_P^{bs\mu\mu} \simeq -0.064$ and $\simeq 0.00$ correspond, respectively, to non-SM and SM solutions, which also exhibit in the $(X^{\rm LR}_{22}, X^{\rm RL}_{32})$ and $(\Delta a_\mu, X^{\rm LR}_{22})$ panels. The non-SM and SM solutions require

$$\frac{X^{\rm RL}_{32}(X^{\rm LR}_{22})^*}{m^2_{V_2}} \simeq \frac{-5.1\times 10^{-5}}{(1\,{\rm TeV})^2} \quad \text{and} \quad \frac{|X^{\rm RL}_{32}(X^{\rm LR}_{22})^*|}{m^2_{V_2}} \lesssim \frac{10^{-5}}{(1\,{\rm TeV})^2}, \tag{4.4}$$

respectively. On the other hand, the $B_s \to e^+e^-$ observable, which is consistent with the SM, sets limit on

$$\frac{|X^{\rm RL}_{31}(X^{\rm LR}_{21})^*|}{m^2_{V_2}} \lesssim \frac{10^{-4}}{(1\ {\rm TeV})^2}, \tag{4.5}$$

explaining the region in the $(X^{\rm LR}_{21}, X^{\rm RL}_{31})$ panel in Fig. 1.

BP-1 fits well to R_{K,K^*}, R_{D,D^*}, $B_s \to \ell^+\ell^-$, and LFV observables; however, it does not induce sizable Δa_μ or Δa_e. BP-2 intriguingly provides simultaneous solutions to Δa_μ and $\Delta a_e^{\rm B}$, as well as a decent fit to B-physics observables. The severe restriction from $\mu \to e\gamma$ is the main difficulty to a generate sizable Δa_μ. Specifically, the former is related to the linear combinations of $X^{\rm LR}_{31}X^{\rm RL}_{32}$ and $X^{\rm LR}_{32}X^{\rm RL}_{31}$, while the latter is related to the product $X^{\rm LR}_{32}X^{\rm RL}_{32}$. Therefore, suppressing the $X^{\rm LR,RL}_{31}$ to avoid the $\mu \to e\gamma$ constraint may help to unleash a large enough Δa_μ. According to Eqs. (4.2) and (4.5), apparently, the above scenario can be achieved by a large enough $|X^{\rm LR}_{21}|$, and this is the main result of BP-2. Unfortunately, the minimum requirement of $|X^{\rm LR}_{21}|$ is significantly above the perturbative limit, $\sqrt{4\pi}$. For example, it needs $X^{\rm LR}_{21} \lesssim -8$ from the $(X^{\rm LR}_{21}, \Delta a_\mu)$ panel in order to start overlapping with the 2σ region of $(g-2)_\mu$, and it is $X^{\rm LR}_{21} = -17.85$ for BP-2. Finally, BP-3 provides an alternative solution for $\Delta a_e^{\rm LKB}$ and B anomalies; meanwhile, it is consistent with LFV and B-physics limits.

The raising of the W-boson mass due to the mass splitting of the isodoublet V_2 is given in Eq. (3.16). The raise depends only on the absolute of the mass difference and is shown in Fig. 2. It can be seen that a mass splitting of 25–30 GeV provides a viable solution to the W-boson anomaly. Such a mass splitting corresponds to 1.25%–1.5% of a 2 TeV LQ.

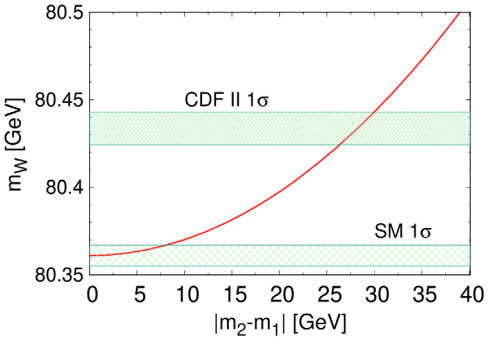

FIG. 2. The resulting W-boson mass due to the mass splitting between the upper and lower isospin components of the vector LQ V_2 around 2 TeV. Note that the lower band in green is the SM prediction, while the upper band is the latest CDF measurement.

V. CONCLUSIONS

Most works in the literature on solving the R_{K,K^*} anomaly rely on reducing $b \to s\mu^+\mu^-$ with the LQ couplings to the left-handed muon. Nevertheless, it remains an almost equally viable solution of increasing $b \to se^+e^-$. Here, in this work, we have attempted to use the isodoublet vector LQ V_2 that couples to the right-handed electron to increase $b \to se^+e^-$ and found parameter space to explain the R_{K,K^*}. Simultaneously, it can also explain the R_{D,D^*} and is consistent with the B_s decays.

We have also investigated the possibility of explaining the muon anomalous magnetic moment. Such a possibility is severely constrained by the leptonic radiative decay $\ell_i \to \ell_j\gamma$. We have successfully found some parameter space points that can explain all R_{K,K^*}, R_{D,D^*}, B_s decays, LFV, and Δa_μ and $\Delta a_e^{\rm B}$ (see BP-2), though one of the couplings is close to or larger than the perturbative limit.

Furthermore, the isodoublet vector leptoquark V_2 naturally explains the W-boson anomaly with a mass splitting of the order of 25–30 GeV between the isospin components.

ACKNOWLEDGMENTS

We especially thank Wolfgang Altmannshofer for useful discussion on renormalization of Wilson coefficients and Chih-Ting Lu for discussion on W-boson anomaly. K. C. also thanks Wai-Yee and Gum-see Keung for their great hospitality. The research was supported in part by the Ministry of Sciences and Technology with Grants No. MoST-110-2112-M-007-017-MY3 and No. MoST-111-2112-M-007-012-MY3.

Note added.—We came across a number of works in the attempt to explain the W-boson anomaly [20–30].

[1] T. Aaltonen *et al.* (CDF Collaboration), Science **376**, 170 (2022).
[2] R. Aaij *et al.* (LHCb Collaboration), Nat. Phys. **18**, 277 (2022).
[3] R. Aaij *et al.* (LHCb Collaboration), J. High Energy Phys. 08 (2017) 055.
[4] Y. S. Amhis *et al.* (HFLAV Collaboration), Eur. Phys. J. C **81**, 226 (2021).
[5] B. Abi *et al.* (Muon g-2 Collaboration), Phys. Rev. Lett. **126**, 141801 (2021).
[6] S. Borsanyi, Z. Fodor, J. N. Guenther, C. Hoelbling, S. D. Katz, L. Lellouch, T. Lippert, K. Miura, L. Parato, K. K. Szabo *et al.*, Nature (London) **593**, 51 (2021).
[7] T. Aoyama, M. Hayakawa, T. Kinoshita, and M. Nio, Phys. Rev. Lett. **109**, 111807 (2012).
[8] T. Aoyama, T. Kinoshita, and M. Nio, Atoms **7**, 28 (2019).
[9] D. Hanneke, S. Fogwell, and G. Gabrielse, Phys. Rev. Lett. **100**, 120801 (2008).
[10] A. Angelescu, D. Bečirević, D. A. Faroughy, F. Jaffredo, and O. Sumensari, Phys. Rev. D **104**, 055017 (2021).
[11] C. Patrignani *et al.* (Particle Data Group), Chin. Phys. C **40**, 100001 (2016).
[12] M. E. Peskin and T. Takeuchi, Phys. Rev. D **46**, 381 (1992).
[13] W. Altmannshofer and P. Stangl, Eur. Phys. J. C **81**, 952 (2021).
[14] W. Altmannshofer, S. Gori, H. H. Patel, S. Profumo, and D. Tuckler, J. High Energy Phys. 05 (2020) 069.
[15] A. Greljo, Y. Soreq, P. Stangl, A. E. Thomsen, and J. Zupan, J. High Energy Phys. 04 (2022) 151.
[16] C. Hati, J. Kriewald, J. Orloff, and A. M. Teixeira, J. High Energy Phys. 12 (2019) 006.
[17] N. Kosnik, Phys. Rev. D **86**, 055004 (2012).
[18] S. Pokorski, *Gauge Field Theories*, 2nd ed. (Cambridge University Press, Cambridge, 2000).
[19] A. Bhol, S. Sahoo, and S. R. Singh, arXiv:2106.06155.
[20] Y. Z. Fan, T. P. Tang, Y. L. S. Tsai, and L. Wu, arXiv:2204.03693.
[21] C. R. Zhu, M. Y. Cui, Z. Q. Xia, Z. H. Yu, X. Huang, Q. Yuan, and Y. Z. Fan, arXiv:2204.03767.
[22] J. de Blas, M. Pierini, L. Reina, and L. Silvestrini, arXiv:2204.04204.
[23] J. M. Yang and Y. Zhang, arXiv:2204.04202 [Sci. Bull. (to be published)].
[24] P. Athron, A. Fowlie, C. T. Lu, L. Wu, Y. Wu, and B. Zhu, arXiv:2204.03996.
[25] A. Strumia, arXiv:2204.04191.
[26] F. Arias-Aragón, E. Fernández-Martínez, M. González-López, and L. Merlo, arXiv:2204.04672.
[27] P. Athron, M. Bach, D. H. J. Jacob, W. Kotlarski, D. Stöckinger, and A. Voigt, arXiv:2204.05285.
[28] J. J. Heckman, arXiv:2204.05302.
[29] K. Sakurai, F. Takahashi, and W. Yin, arXiv:2204.04770.
[30] C. T. Lu, L. Wu, Y. Wu, and B. Zhu, arXiv:2204.03796.